JOURNAL OF MATERIALS SCIENCE 27 (1992) 4619–4624

# Photoelectrochemical reactions on semiconductor materials

## Part I *Influence of electrode surface activation on the reduction of oxidants on an n-GaAs electrode*

O. SAVADOGO
*Département de métallurgie et de génie des matériaux, École Polytechnique de Montréal, C. P. 6079, succ. "A", Montréal, Quebec, Canada H3C 3A7*

The cathodic reduction of $Fe^{3+}$ ions and $I_2$ on an *n*-GaAs electrode was studied. The variation in the current density with the concentration of the oxidant has been interpreted as being the result of a reduction mechanism involving interface or surface states, an interpretation that is amply substantiated by experimental data. The effect of the surface modification with $SiW_{12}O_{40}^{4-}$ on the reduction process was studied. Prior to this electrode activation, the rate constant for electrons being transferred from the conduction-band to the interface or surface states, $k_S$, was observed to be independent of electrode potential, whereas in the case of the modified *n*-GaAs, $k_S$ depends on band-bending. On the other hand, the rate constant for electrons being transferred from the interface or surface states to oxidant species, $k_{ox}$, does depend on electrode potential in the case of the unmodified n-GaAs, and is independent of band-bending in the case of the modified *n*-GaAs. This change may be attributed to the filling of the active surface or interface states or their redistribution after the electrode surface activation.

## 1. Introduction

The key problems associated with the use of photoelectrochemical (PEC) devices for the conversion and storage of solar energy are electrode instability and the low-rate and irreversible charge transfer at the interface [1–5]. We have recently shown [6] that the modification of several semiconductor material surfaces with $H_4SiW_{12}O_{40}{\cdot}nH_2O$ produces an increase in open-circuit photopotential at the semiconductor/electrolyte interface, $V_{OC}$, without changing the flat-band potential but while still maintaining good photoelectrode stability. In view of these interesting properties, PEC devices appear to be valuable candidates for the conversion and storage of high energy. The next step is to investigate other photoelectrochemical reactions on these electrodes involving non-polluting and easily manipulated redox systems.

Ferricyanide reactions at the GaAs/electrolyte interface have been studied [7–12], and it is known that the process of reducing $[Fe(CN)_6]^{3-}$ involves carriers via the valence band in a basic medium. We have described elsewhere [12] the experimental conditions required in preparing the electrodes to ensure good reproducibility of the current–potential characteristics at the interface during the reduction of $[Fe(CN)_6]^{3-}$ in a basic medium, and the influence of the surface states on the current–potential curves has been determined. Accordingly, the reduction of $[Fe(CN)_6]^{3-}$ on the *n*-GaAs electrode is influenced by the surface or interface state of the material, i.e. the reaction is not purely diffusion controlled. The activation component of the current density due to the surface states increases as the electrode potential decreases, although we have also shown that under illumination the cathodic current decreases if ferrocyanide is present in the electrolyte. This result has been attributed to the oxidation of $[Fe(CN)_6]^{4-}$ which involves the minority carriers (*p*) via the valence-band. This was possible because, in alkaline solutions, e.g. pH = 12, the flat-band potential of *n*-GaAs ($n \sim 10^{17}\,cm^{-3}$) was $-1.75$ V versus the saturated calomel electrode (SCE). Furthermore the $[Fe(CN)_6]^{4-/3-}$ energy level lay outside the energy gap.

This paper presents the results of a study on the reduction of $Fe^{3+}$ or $I_2$ on n-GaAs in an aqueous solution. For comparison purposes, the reduction of these oxidants on the modified *n*-GaAs electrode was studied to try to establish the role of the derivatization process in the photoelectrochemical charge transfer phenomenon in determining the behaviour of this electrode.

## 2. Experimental procedure

The reference electrode was a saturated calomel electrode (SCE), the counter electrode was a large-surface-area platinum gauze, and the working electrode was

0022–2461 

monocrystalline *n*-GaAs with a doping density of $\sim 10^{17}$ cm$^{-3}$ and a surface area of 0.1 cm$^2$. In successive steps, samples were degreased with trichloroethylene for 30 s, mechanically polished with a 1 μm diamond paste, chemically etched in $H_2SO_4$ (concentrated) + $H_2O_2$ (30%) for 10 s, and rinsed in distilled water. The electrode was re-treated as above between runs.

Each experiment to determine current–potential characteristics was carried out at least three times to ensure the reproducibility of the data.

### 2.1. Electrochemical equipment and apparatus

The capacitance of the electrode/electrolyte interface at various electrode potentials was measured with a PARC frequency response analyser (Model 378) and a PARC electrochemical interface (Model 276). The current–potential characteristics of the electrode/electrolyte interface at various electrode potentials were measured with a PARC Universal Programmer analyser (Model 270) and a PARC electrochemical interface (Model 276).

The polarization curves were obtained using a two-compartment cell with 100 ml capacity and a standard three-electrode configuration. Reagent-grade $FeCl_2$, $FeCl_3$, $I_2$, KI, $H_2SO_4$ and HCl were used for the capacitance measurements and the current–potential characteristics. 12-tungsten-silicon ($SiW_{12}O_{40}^{4-}$) heteropolyacid was also used. The solutions were deoxygenated thoroughly with nitrogen, and kept under a positive pressure of this gas throughout the experiments.

During all the experiments, the solutions were mechanically stirred.

## 3. Results and discussion

### 3.1. Electrode derivatization and electrocatalysis

In acidic solutions (pH = 0), experiments performed on a glassy carbon electrode indicated that five reduction waves may be observed, located respectively at $-0.265$, $-0.490$, $-0.83$ and $-0.930$ V/SCE ([13–16] and references therein). This is evidence that a negative potential can be used to achieve the electrode surface modification with $SiW_{12}O_{40}^{4-}$.

The material surfaces were modified by a method fully described elsewhere ([6] and references therein). Briefly, the supporting electrolyte for the electrode derivatization was 1 M $H_2SO_4$, which contained $5 \times 10^{-4}$ M $H_4SiW_{12}O_{40} \cdot nH_2O$ in a nitrogen atmosphere. The modifications were achieved under potentiostatic conditions with a negative potential ($-1.2$ V/SCE).

During the derivatization process, the observed current gradually increased with the evolution of the gas. The derivatization time ($\sim 45$ min) was determined once the current had been stabilized. The current increase is attributed to the activation process of the electrode which undergoes an improvement of the hydrogen evolution reaction. ESCA and XPS analysis of the chemical composition of the electrode surface revealed the presence of silicon and tungsten. Analogous results were obtained on palladium, platinum and nickel electromodified electrodes [17, 18]. The number of tungsten atoms per cm$^2$ were measured by the Rutherford back-scattering technique after surface modification. The number of silicon and tungsten atoms is $1.5 \times 10^{15}$ cm$^{-2}$ and $5 \times 10^{14}$ cm$^{-2}$, respectively.

The SEM observations show that the morphological difference between modified and unmodified electrodes is the presence of numerous microscopic particles on the activated surfaces. On the modified electrodes, there are large aggregates of these particles ($\geqslant 4$ μm), irregularly distributed. These observations agree well with the results of Rutherford's backscattering technique which show a significant quantity of silicon and tungsten atoms per surface unit after the electrode surface modification was achieved.

### 3.2. Determination of the energy levels of the electrodes

The energy levels of the material were determined from a knowledge of the flat-band potential, $V_{fb}$, which was deduced from impedance measurements. Using results that we obtained recently on the same electrodes [6], it was found that plots of $C^{-2}$ versus $V$ are straight lines in a large potential interval ($\geqslant 1$ V) and over a wide frequency range (1–12 kHz). In fact, the same extrapolated value of $V_{fb}$ is obtained over this frequency range. Thus the Schottky–Mott (S–M) model is verified for these interfaces, i.e. the following equation applies:

$$\frac{1}{C^2} = \frac{2}{e\,\varepsilon\,\varepsilon_0\,N}\left(V - V_{fb} - \frac{kT}{e}\right) \qquad (1)$$

where $C$ is the interface capacitance per unit area, $e$ the electron charge ($1.6 \times 10^{-19}$ c), $\varepsilon$ the semiconductor dielectric constant, $\varepsilon_0$ the vacuum permittivity ($8.85 \times 10^{-14}$ F cm$^{-1}$), and $N$ the donor (*n*-type) density. From this measurement, $V_{fb}$ was determined with an accuracy of $\pm 0.100$ V.

A flat-band potential of $V_{fb} = -0.80$ V/SCE is obtained for modified electrodes by bringing 1 M HCl in contact with $5 \times 10^{-4}$ M $Fe^{3+/2+}$. In 1 M HCl without $Fe^{3+/2+}$, the same value of $V_{fb}$ is obtained [6]. Because illumination of the interfaces with a light-power input of 50 mW cm$^{-2}$ has no effect on $V_{fb}$, the results obtained under illumination are not shown here. Experimental results show, however, that the presence of the $I_2/I^-$ redox system in the electrolyte gives a flat-band potential value of $-0.82$ V/SCE. The energy diagrams of the electrodes are shown in Fig. 1 with $Fe^{3+/2+}$ and $I_2/I^-$ as the redox systems. For a large number of redox systems, the $V_{redox}$ of which span a range of 2.1 V [6], a variation of $V_{fb}$ with $V_{redox}$ was observed on unmodified electrodes while a non-variation of $V_{fb}$ with $V_{redox}$ was observed on modified electrodes. On the other hand, in 1 M HCl, $V_{fb}$ has the same value on both modified or unmodified electrodes.

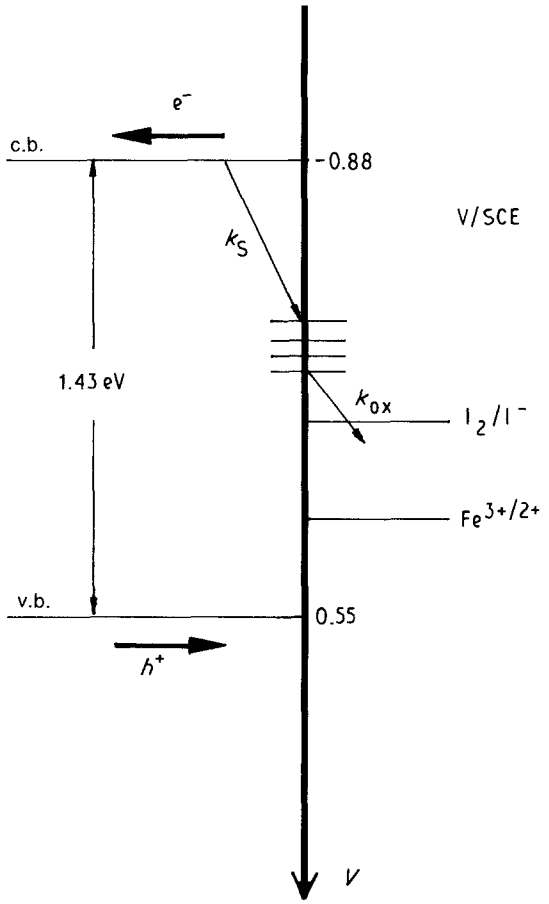


*Figure 1* Energy diagrams of the *n*-GaAs/1 M HCl with $Fe^{3+/2+}$ or $I_2/I^-$ as redox systems. c.b. is conduction band and v.b. is valence band.

With a knowledge of the flat-band potential, it is possible to determine the energy-level positions at the semiconductor/electrolyte interface by using the classical relation between the valence-band energy, $E_{vb}$, the conduction-band energy, $E_{cb}$ and the flat-band energy, $E_{fb}$. For the *n*-type semiconductor, $E_{cb}$ is related to $E_{fb}$ by the classical relation

$$E_{cb} - E_{fb} = kT\log\left(\frac{n}{N_c}\right) \quad (2)$$

where $n$ is the doping density of the semiconductor and $N_c$ the effective density of states in the conduction-band. For the GaAs samples used here, $N_c$ is 4.7 $\times 10^{17}$ cm$^{-3}$ [19] and $n$ is $\sim 10^{17}$ cm$^{-3}$. Using these values of $n$ and $N_c$ in Equation 2, we find that the difference between $E_{cb}$ and $E_{fb}$ is 0.08 eV. Furthermore, the flatband potential can be shown to be at the bottom of the conduction band, i.e. the conduction-band edge lies at 0.88 eV relative to the calomel reference energy.

With a GaAs bandgap of 1.43 eV, the valence band is at − 0.55 eV. The energy levels, $E^{\circ}_{redox}$, of the simple ions in the solution used here, such as $Fe^{3+}/Fe^{2+}$ or $I_2/I^-$, are estimated directly from their redox potential, $E^0$. Furthermore, the $E^{\circ}_{redox}$ value of $Fe^{3+}/Fe^{2+}$ and $I_2/I^-$ will be approximately − 0.45 and − 0.30 eV, respectively, relative to the calomel energy. The Fermi energy of the calomel reference electrode will be about − 0.24 eV relative to the zero of energy (the Handbook gives $E^0 = 0.24$ V for calomel). Furthermore, the band positions at the semiconductor/electrolyte interface are shown in Fig. 1.

### 3.3 Study on electrodes without derivatization

It should be pointed out that previous experiments carried out with similar electrodes in the same medium but without modification of their surfaces [6], have shown Fermi-level pinning due to the presence of a high density of surface states. Accordingly, the band edges at the semiconductor/electrolyte interface varied as a function of the different redox couples, the $V_{redox}$ of which span a range of 2.1 V, whereas the open-circuit photopotential of the electrodes, $V_{oc}$, was relatively independent of $V_{redox}$.

Fig. 2 shows the influence of electrode surface modification on the current–potential characteristics of the *n*-GaAs/1M HCl, both in the absence and in the presence of $10^{-3}$ M $Fe^{3+}$. It has been verified that in the absence of $Fe^{3+}$, the electrode surface modification has no effect on its cathodic characteristics in the dark. Furthermore, the same curve (Fig. 2a) is obtained with the two electrodes in contact with HCl and without $Fe^{3+}$.

This behaviour is different from that described in other published data on *p*-type semiconductors where an improvement in the hydrogen evolution reaction was observed after electrode surface modification (see, for example, [6, 13, 20] and references therein).

However, as may be seen in Fig. 2b and c, a large cathodic dark current was observed upon the addition of $Fe^{3+}$. The excess cathodic dark current obtained with the modified electrode is more important than that obtained with the bare electrode. According to the energy diagrams of the *n*-GaAs/electrolyte interface (see Fig. 1), this current can be explained by electron transfer from the conduction band. Consequently, we have to find a model for this process to explain, for example, how electrons from the bulk of the GaAs reach its surface. The excess cathodic current density, $\Delta i_c$, due to the reduction of $Fe^{3+}$ (ox) was used to determine the kinetics of the reaction. $\Delta i_c$ is the

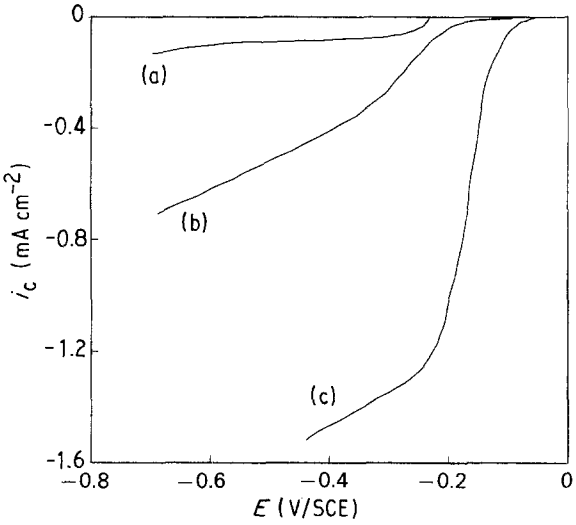


*Figure 2* Cathodic current–potential curves of the n-GaAs/1 M HCl when the electrode is bare (a), (b) reduction of $Fe^{3+}$ on the bare electrode, and (c) reduction of $Fe^{3+}$ on a modified n-GaAs.

TABLE I Variation of the parameters of Equation 5 for the reduction of $Fe^{3+}$ on an unmodified *n*-GaAs. Data from Fig. 2

| $V$ (V/SCE) | $b$ ($10^{-3}$ $A^{-1}$ $cm^{-2}$) | $k_S$ ($10^{16}$ $cm^3$ $s^{-1}$) | $a$ ($A^{-1}$ $cm^2$ M) | $k_{ox}$ ($10^{-4}$ $M^{-1}$ $cm^2$) | $f$ (for $C_{ox} = 10^{-3}$ M) |
|---|---|---|---|---|---|
| − 0.6 | 1 | 1.32 | 1.00 | 6.25 | 0.60 |
| − 0.5 | 1 | 1.32 | 1.56 | 4.00 | 0.68 |
| − 0.4 | 1 | 1.32 | 2.00 | 3.12 | 0.80 |
| − 0.3 | 1 | 1.32 | 3.00 | 2.08 | 0.82 |

difference between the cathodic current density with ox and without ox. Typical examples of the excess cathodic current density dependence on the concentration of $Fe^{3+}$, $C_{ox}$, are shown in Fig. 3. The magnitude of the current is close to that expected for a diffusion-controlled reaction. As may be seen, $\Delta i_c$ does not increase linearly with $C_{ox}$. Furthermore, the curvature of the plots could be taken as evidence of the absence of diffusion control. On the other hand, it was also observed that neither the amount of $Fe^{2+}$ ($C_{red}$) nor illumination has any effect on $\Delta i_c$, and therefore these results are not shown. Finally, the reduction rate is not affected by temperature. As may be seen in Fig. 1, the energy levels of $I_2/I^-$ and $Fe^{3+/2+}$ are far from the conduction band. This indicates that the reduction of $Fe^{3+}$ by the conduction-band electrons must involve interface states. A similar strategy has also been applied to the reduction of $[Fe(CN)_6]^{3-}$ on $TiO_2$ and $SrTiO_3$ [21], $Fe_2O_3$ [22] and $CdIn_2S_4$ [23] in a basic medium.

The rate of electrons being transferred from the conduction band to the interface states is given by

$$\frac{dn_e}{dt} = k_S N_c (1 - f) N_S \tag{3}$$

where $N_c$ is the electron density of the conduction band, $N_S$ is the density of the interface or surface states, $k_S$ the rate constant for the electron transfer from the conduction band to the interface states, and $f$ the occupation factor of these states. Hence, the rate of electrons being transferred to ox is given by

$$\frac{dn_e}{dt} = k_{ox} f N_S C_{ox} \tag{4}$$

where $k_{ox}$ is the rate constant for the electron transfer from the interface states to $Fe^{3+}$, and $C_{ox}$ the concentration of $Fe^{3+}$.

Using Equations 3 and 4, we obtain

$$\Delta i_c = e\frac{dn_e}{dt} \tag{5}$$

or

$$\frac{1}{\Delta i_c} = \frac{1}{eN_S}\left(\frac{1}{k_S N_C} + \frac{1}{k_{ox} C_{ox}}\right) \tag{6a}$$

or

$$\frac{1}{\Delta i_c} = a\frac{1}{C_{ox}} + b \tag{6b}$$

with

$$a = \frac{1}{N_S e k_{ox}} \tag{7a}$$

$$b = \frac{1}{N_S e k_S N_C} \tag{7b}$$

As may be seen in Fig. 4, the replotted data of Fig. 3 representing $1/\Delta i_c$ versus $1/C_{ox}$ are straight lines. Thus, the experimental results are satisfactorily explained by Equation 6. From the intercept with the $1/\Delta i_c$ axis, the values of $b$ are obtained. The values of $a$, $b$ and $f$ deduced from Fig. 4 are summarized in Table I. As indicated, in the range of potential investigated here, the value of $b$ is constant and is given by

$$1/b = e N_S k_S N_C = 10^{-3}\,A^{-1}\,cm^{+2} \tag{8}$$

e.g. $N_S k_S N_C = 6.25 \times 10^{15}\ cm^{-2} s^{-1}$. Assuming that

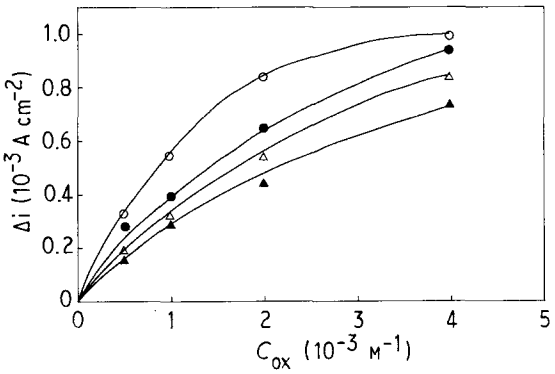


*Figure 3* Excess cathodic dark current density, $\Delta i_c$, at the base *n*-GaAs electrode as a function of the concentration of ferric ions, $C_{ox}$, in 1 M HCl.

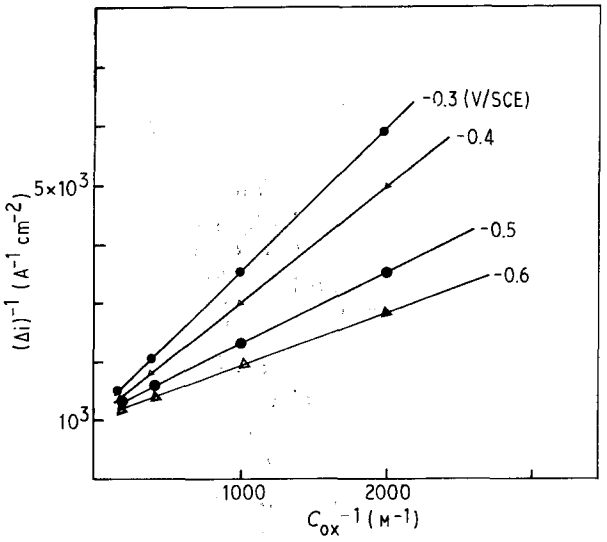


*Figure 4* Reciprocal excess cathodic dark current density ($1/\Delta i_c$) versus reciprocal concentration of $Fe^{3+}$ ($1/C_{ox}$) in 1 M HCl for an unmodified *n*-GaAs.

TABLE II Variation of the parameters of Equation 6 for the reduction of $Fe^{3+}$ in 1 M HCl on a modified *n*-GaAs. Data from Fig. 3

| $V$ (V/SCE) | $b$ ($A^{+1}\,cm^{-2}$) | $k_S$ ($10^{16}$ $cm^{73}\,S^{-1}$) | $a$ ($10^2$ $A^{-1}\,cm^2\,M$) | $k_{ox}$ ($10^{-5}$ $M^{-1}\,cm^2$) | $f$ (for $C_{ox} = 10^{-3}$ M) |
|---|---|---|---|---|---|
| − 0.6 | 200 | 6.63 | 25 | 2.5 | 0.5 |
| − 0.5 | 294 | 4.51 | 25 | 2.5 | 0.5 |
| − 0.4 | 400 | 3.31 | 25 | 2.5 | 0.5 |
| − 0.3 | 500 | 2.65 | 25 | 2.5 | 0.5 |

$N_S$ has the dimensions of a surface ($cm^{-2}$) and $N_C$ has those of a volume ($cm^{-3}$), $k_S$ is then expressed in dimensions of $cm^3\,S^{-1}$. If, on the other hand, we assume that $N_C$ and $N_S$ have values of $4.7 \times 10^{17}$ $cm^{-3}$ and $10^{14}$ $cm^{-2}$ [24], respectively, then $k_S = 1.32 \times 10^{-16}$ $cm^3\,s^{-1}$, i.e. 13.2 $nm^3\,s^{-1}$. As may be seen in Table I, the values of, for example, the slopes of the curves in Fig. 4 vary quite remarkably with the electrode potential. They yield values of $k_{ox}$. These values vary from $6.25 \times 10^4$ to $2.08 \times 10^4$ $M^{-1}\,cm^2$ depending on the electrode potential (see Table I) and the variation in the occupation factor, $f$, of the interface states. As indicated, $f$ increases, as expected, with potential, whereas $k_{ox}$ decreases as potential increases. This indicates that the reduction is not purely diffusion controlled. The reaction could have an important activation component of the electrochemical reaction process. This phenomenon may be attributed to the influence of the surface states or interface states on the electrochemistry of this reaction. This is in agreement with other published data (see, for example [6, 25–28]) which have indicated that the surface or interface states have an important effect on the photoelectrochemical reactions at the semiconductor/electrolyte interface. However, the rate constant for the electron transfer from the conduction band to the interface states is independent of the electrode potential, whereas the rate constant for the electron transfer from the interface states to the redox system changes with the electrode potential. This can be attributed to the presence of charged traps in the interface states. Consequently, the concept of Fermi-level pinning was used to explain these experimental results based on a so-called "surface-controlled model", e.g. $V_{fb}$ will (and does) change with $V_{redox}$, whereas $V_{oc}$ (the open-circuit photopotential) is independent of $V_{redox}$ ([6, 25–28] and references therein). Support for this influence can be found by studying the reduction of $Fe^{3+}$ under experimental conditions where the suppression of the Fermi-level is achieved. These results are discussed in the following section.

### 3.4. Study of electrodes activated with $H_4SiW_{12}O_{40}\cdot nH_2O$

As our recently published data [6] have shown, a suppression of Fermi-level pinning on the n-GaAs electrode is obtained after modifying the electrode surface with $H_4SiW_{12}O_{40}\cdot nH_2O$. In other words, with the presence of a large number of redox systems in the electrolyte, the $V_{redox}$ of which span a range of 2.1 V, the open-circuit photopotentials, $V_{oc}$, of the modified electrodes vary with $(V_{fb} - V_{redox})$ with a slope of unity.

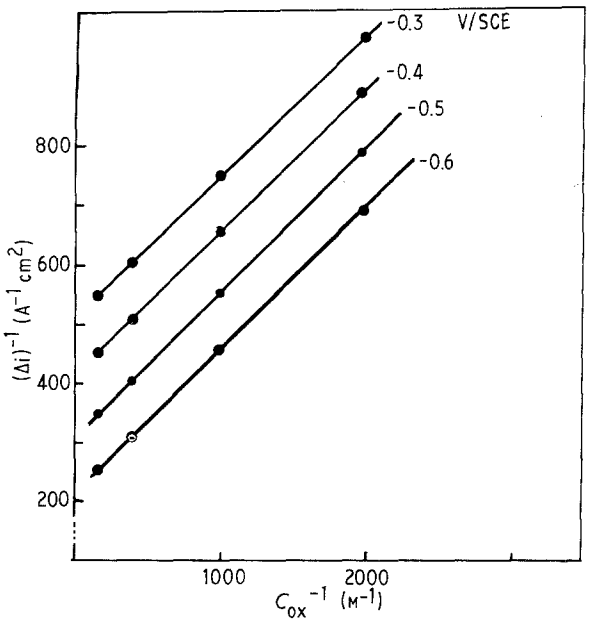


*Figure 5* Variation of $(1/\Delta i_c)$ with $(1/C_{ox})$ in 1 M HCl for a modified n-GaAs with $H_4SiW_{12}O_{40}\cdot nH_2O$.

The variation in the excess cathodic current density with the concentration of $Fe^{3+}$ is shown in Fig. 5. As may be seen, $1/\Delta i_c$ is a linear function of $1/C_{ox}$. Plots of $(\Delta i_c)^{-1}$ versus $C_{ox}^{-1}$ are parallel straight lines for different electrode potentials. These results may also be explained using Equations 5 and 6. The corresponding values of $a$, $b$ and $f$ deduced from Fig. 5 are summarized in Table II. These values may be compared to those in Table I. As indicated, the intercept with the $1/\Delta i_c$ axis increases with the potential. In this case, therefore, the rate constant $k_S$, which was expected to depend on the band bending, in effect varies with the electrode potential. However, in the same range of potential investigated, the value of $k_S$ is higher for modified electrodes ($\sim 10^{-15}$ $cm^3\,s^{-1}$) than for unmodified electrodes ($\sim 10^{-16}$ $cm^3\,s^{-1}$). Also, a value of $k_{ox}$ ($2.50 \times 10^5$ $M^{-1}\,cm^2$) independent of the electrode potential is obtained which is higher than that recorded in Table I ($\sim 10^4$ $M^{-1}\,cm^2$ versus $\sim 10^5$ $M^{-1}\,cm^2$). Thus, in this case, $f$ does not change with the electrode potential (see Table II). These results may be attributed to an increase of the filling of the active interface states or/and their redistribution after the electrode surface modification. If we assume that $N_C$ has the same value as above ($\sim 4.7 \times 10^{17}$ $cm^{-3}$), then the increase in $k_S$ for the modified *n*-GaAs electrode agrees well with this conclusion. Another factor in support of this conclusion may be found through studying the reduction of $I_2$ on the

TABLE III Variation of the parameters of Equation 5 for the reduction of $I_2$ in 1 M HCl on an unmodified and on a modified *n*-GaAS

| | *n*-GaAs electrode | | | |
|---|---|---|---|---|
| | Unmodified | | Modified with $H_4SiW_{12}O_{40}{\cdot}nH_2O$ | |
| *V* (V/SCE) | *b* ($10^{-3}$ $A^{+1}$ $cm^2$) | *a* ($A^{-1}$ $cm^2$ M) | *b* ($A^{+1}$ $cm^{-2}$) | *a* ($10^2$ $A^{-1}$ $cm^2$ M) |
| − 0.6 | 1 | 1.10 | 100 | 25 |
| − 0.5 | 1 | 1.55 | 200 | 25 |
| − 0.4 | 1 | 2.01 | 300 | 25 |
| − 0.3 | 1 | 3.05 | 405 | 25 |

modified and on the unmodified *n*-GaAs electrodes. Experimental results show that this reduction process is also described by the model stated in Equations 6a and b. The corresponding parameters, *a* and *b*, are summarized in Table III. In the case of the unmodified electrodes, the value of *b* does not change from $Fe^{3+}$ to $I_2$. On the contrary, for the modified electrode, the value of *b* is smaller for the reduction of $I_2$ than for that of $Fe^{3+}$. In other words, the modification of the electrode surface shows that in the case of $k_S$, for example, the excess current density increases from $I_2$ to $Fe^{3+}$ (see Tables II and III). This change is not observed in the case of unmodified electrodes. These results indicate that surface modification induces changes in the excess current density caused by the change of $K_S$.

## 4. Conclusion

Based on the results reported here, it may be concluded that the reduction of $Fe^{3+}$ and $I_2$ can be described by a simple model involving a two-step process via interface states. It has also been shown that the activation of the semiconductor electrode with $H_4SiW_{12}O_{40}{\cdot}nH_2O$ modifies the reduction process. Prior to electrode activation, the rate constant for electrons being transferred from the conduction-band to the interface surface states, $k_S$, was observed to be independent of the electrode potential, whereas, on the modified *n*-GaAs electrode, $k_S$ depends on band bending. On the other hand, the rate constant for electrons being transferred from the interface or surface states to oxidant species, $k_{ox}$, does depend on electrode potential in the case of the unmodified *n*-GaAs electrode, whereas it was independent of band bending for the modified *n*-GaAs. This change may be attributed to the increase of the filling of the active surface states or/and their redistribution after the electrode surface modification with $SiW_{12}O_{40}{\cdot}26\ H_{20}$.


## Acknowledgements

The author thanks the "Fonds FCAR-Actions structurantes" of the Quebec Government, and the Natural Science and Engineering Research Council of Canada, for their financial support.


## References


1. K. RAJESHWAR, P. SINGH and J. DUBOW, *Electrochem. Acta* **23** (1978) 1117.
2. G. HODES, J. MANASSEN and D. CAHEN, *Nature* **261** (1976) 403.
3. J. MANASSEN, G. HODES and D. CAHEN, *J. Electrochem. Soc.* **124** (1977) 532.
4. P. G. ANG and A. F. SAMMELS, *Faraday Discuss. R. Soc. Chem.* **70** (1980) 207.
5. S. R. MORISSON, "Electrochemistry on Semiconductors and Oxidized metals" (Plenum Press, New York, 1980).
6. O. SAVADOGO, *Can. J. Chem.* **67** (1989) 382.
7. H. GERISCHER and I. MOTTES, *S. Phys. Chem. Neue, Falge* **49** (1966) 112.
8. H. GERISCHER, *Ber. Bunsenges Phys. Chem.* **69** (1965) 578.
9. K. H. BECKMAN and R. MEMMING, *J. Electrochem. Soc.* **116** (1969) 368.
10. R. MEMMING and G. SCHWANDT, *Electrochem. Acta* **13** (1968) 1299.
11. W. L. LAFFERE, F. CARDON and W. P. GOMES, *Surf. Sci.* **44** (1974) 451.
12. O. SAVADOGO and A. DESCHANVRES, *Bull. Soc. Chim. Fr.* **I** (1983) 233.
13. B. KEITA and L. NADJO, *J. Electroanal. Chem.* **191** (1985) 441.
14. G. HERVÉ, *Ann. Chim. Paris* **6** (1971) 219.
15. *Idem. ibid.* **6** (1971) 287.
16. J. M. FRUCHART and G. HERVÉ, *ibid.* **6** (1971) 337.
17. O. SAVADOGO, in "Proceedings of the 13th International Precious Metals Institute (IPMI)", (Harris, IPMI Allentown, USA, 1989) pp. 75–8.
18. O. SAVADOGO and D. L. PIRON, *Int. J. Hydrogen Energy* **15** (1990) 715.
19. S. M. SZE, "Physics of Semiconductor Devices" (Wiley, New York, 1981) p. 850.
20. G. S. POPKIROR, A. YA. SAKHAROVA and YU. PLESKOV, *Int. J. Hydrogen Energy* **13** (1988) 681.
21. J. VANDERMOLEN, W. P. GOMES and F. CARDON, *J. Electrochem. Soc.* **127** (1980) 324.
22. P. IWANSKI, J. S. CURRAN, W. GISSLER and R. MEMMING, *ibid.* **128** (1981) 2128.
23. O. SAVADOGO. to be published.
24. S. M. SZE, "Physics of Semiconductor Devices" (Wiley, New York, 1981) p. 275.
25. F. R. FAN and A. J. BARD, *J. Amer. Chem. Soc.* **10** (1980) 3677.
26. J. J. KELLY and R. MEMMING, *J. Electrochem. Soc.* **129** (1982) 730.
27. D. VANNEACHELBERGH, W. P. GOMES and F. CARDON, *Ber. Bunsenges. Phys. Chem.* **89** (1985) 994.
28. R. MEMMING, *ibid.* **91** (1987) 353.



*Received 4 March*
*and accepted 8 May 1991*